HHS Public Access

Author manuscript

Clin Nucl Med. Author manuscript; available in PMC 2018 October 01.

Published in final edited form as:

Clin Nucl Med. 2017 October ; 42(10): 741–748. doi:10.1097/RLU.0000000000001752.

Assessment of Organ Dosimetry for Planning Repeat Treatments of High-Dose ^{131}I-MIBG Therapy: ^{123}I-MIBG vs. Post-Therapy ^{131}I-MIBG Imaging

Neeta Pandit-Taskar, MD[1,*], **Pat Zanzonico, PhD**[2], **Patrick Hilden, MS**[3], **Irina Ostrovnaya, PhD**[3], **Jorge A. Carrasquillo, MD**[1], and **Shakeel Modak, MD**[4]

[1]Molecular Imaging and Therapy Service, Department of Radiology, Memorial Sloan Kettering Cancer Center, New York, NY

[2]Department of Medical Physics, Memorial Sloan Kettering Cancer Center, New York, NY

[3]Department of Epidemiology and Biostatistics, Memorial Sloan Kettering Cancer Center, New York, NY

[4]Department of Pediatrics, Memorial Sloan Kettering Cancer Center, New York, NY

Abstract

Purpose—To evaluate detailed organ-based radiation absorbed dose for planning double high-dose treatment with ^{131}I-MIBG.

Materials and Methods—In a prospective study, 33 patients with high-risk refractory or recurrent neuroblastoma were treated with high-dose ^{131}I-MIBG. Organ dosimetry was estimated from first ^{131}I-MIBG post-therapy imaging and from subsequent ^{123}I-MIBG imaging prior to the planned second administration. Three serial whole-body scans were performed per patient 2–6 days post-^{131}I-MIBG therapy (666 MBq/kg or 18mCi/kg) and approximately 0.5, 24, and 48 hours after the diagnostic ^{123}I-MIBG dose (370 MBq/kg or 10mCi/1.73m^2). Organ radiation doses were calculated using OLINDA. ^{123}I-MIBG scan dosimetry estimations were used to predict doses for the second ^{131}I-MIBG therapy and compared with ^{131}I-MIBG post-therapy estimates.

Results—Mean ± SD whole-body doses from ^{131}I-MIBG and ^{123}I-MIBG scans were 0.162±112 and 0.141±0.068 mGy/MBq, respectively. ^{123}I-MIBG and ^{131}I-MIBG organ doses were variable—generally higher for ^{123}I-MIBG projected doses than those projected using post-therapy ^{131}I-MIBG scans. Mean ± SD doses to liver, heart wall, and lungs were 0.487±0.28, 0.225±0.20, and 0.40±0.26, respectively for ^{131}I-MIBG and 0.885±0.56, 0.618±0.37, and 0.458±0.56, respectively, for ^{123}I-MIBG. Mean ratio of ^{123}I-MIBG to ^{131}I-MIBG estimated radiation dose was 1.81±1.95 for liver, 2.75±1.84 for heart, and 1.13±0.93 for lungs. No unexpected toxicities were noted based on ^{123}I-MIBG projected doses and cumulative dose limits of 30, 20, and 15 Gy to liver, kidneys, and lungs, respectively.

[*]Corresponding Author: Neeta Pandit-Taskar, MD, 1275 York Avenue, Box 77, New York, NY 10065, pandit-n@mskcc.org, Phone: +1 (212) 639-3046, Fax: +1 (212) 717-3263.

Conflict of Interest: The authors report no conflict of interest. This research was funded in part through the NIH/NCI Cancer Center Support Grant P30 CA008748, particularly the MSK Biostatistics core.

Conclusions—For repeat ^{131}I-MIBG treatment planning, both ^{131}I-MIBG and ^{123}I-MIBG imaging yielded variable organ doses. However, ^{123}I-MIBG-based dosimetry yielded a more conservative estimate of maximum allowable activity and would be suitable for planning and limiting organ toxicity with repeat high-dose therapies.

Keywords

^{123}I-MIBG; ^{131}I-MIBG; dosimetry; MIBG therapy; therapy planning; neuroblastoma

BACKGROUND

^{131}I-MIBG therapy (MIBG therapy) is increasingly being used in the treatment of patients with chemo-refractory or relapsed neuroblastoma (NB), a pediatric malignancy associated with poor prognosis. ^{123}I-MIBG imaging is a mainstay assessment and the recommended standard imaging modality for NB.[1–4] The dosing of ^{131}I-MIBG for therapy in neuroblastoma has been based on body weight, with regimens ranging from multiple infusions of low-activity (37–148 MBq/kg or 1–4 mCi/kg) to high-activity MIBG therapy (296–666 MBq/kg or 8–18 mCi/kg); alternatively, some regimens have used fixed doses and others have based dosing based on whole-body dosimetry.[5] Myelosuppression is the most common adverse event and limits the activity that can be administered. However, with the increasing availability of cryopreserved stem cells in patients with NB, high-dose MIBG therapy followed by stem cell rescue to reverse myelosuppression has become the norm for such patients.[6, 7] Other adverse events include transient sialoadenitis, hypertension, and hepatotoxicity.

Response rates, even with high-dose MIBG therapy, are suboptimal; combined therapy with radiation sensitizers has been explored to improve efficacy,[8, 9] and serial high-dose MIBG therapy has been used.[10, 11] High-dose therapies are associated with toxicities and dose amounts to the normal organ is of concern. Dosimetric estimations are used to allow for maximizing activity administration while keeping normal organ doses within tolerable limits to prevent toxicity. Previous studies have primarily used whole-body radiation and red marrow-absorbed dose estimates. In a study that used pretherapy ^{123}I-MIBG imaging to predict whole-body dose for MIBG therapy,[12] whole-body counting without imaging showed large intra-patient variations in estimating whole-body absorbed doses allowing for a maximum 4 Gy total absorbed dose for two doses.[13] Pretreatment ^{131}I-MIBG imaging-derived dose estimates appear to be more reproducible than weight-based dosing; however, it underestimates the therapeutic dose and shows large inter-patient variations in tumor-absorbed dose.[14–16] Furthermore, repeated ^{131}I-MIBG imaging raises concern about increasing radiation exposure in children. Positron emission tomography (PET)-based dosimetry with ^{124}I-MIBG has been performed and allows for organ and body dose estimations, but it is restricted in terms of broad applicability due to the fact that ^{124}I-MIBG is currently not US Food and Drug Administration-approved[17, 18] or universally available, and because radiolabeling requires expertise that limits its use.

While various techniques have been used to assess activity administration, individual organ dosimetry has not been evaluated for planning repeat, tandem MIBG therapy or multiple

MIBG infusions. Assessment of organ doses may help individualize therapy and prevent prohibitive radiogenic side effects, while allowing for administration of the maximum "safe" therapeutic activities in those who respond to first high-dose therapy. This is especially critical in high-activity or repeat therapies with stem cell support where marrow toxicity is not limiting but organ doses may be therapy-limiting; dosimetry will allow for maximizing activity administration while keeping the absorbed dose to individual critical organs such as the lung, liver, and kidney within tolerance limits.

^{123}I-MIBG is now universally available in the US and Europe, and is considered the gold standard for diagnosis and staging of NB. However, its role in radiation dose assessment and particularly organ dosimetry remains largely undetermined. To our knowledge, this is the first study to systematically evaluate ^{123}I-MIBG to estimate individual organ absorbed doses for planning MIBG therapy. We prospectively performed ^{123}I-MIBG and ^{131}I-MIBG organ dosimetry in patients with NB to plan treatment doses and compared the organ dose estimates to evaluate the suitability of ^{123}I-MIBG imaging for treatment planning.

METHODS

Patients

Patients with high-risk refractory or recurrent NB were treated on a phase II single-arm, open-label study approved by our Institutional Review Board (Clinicaltrials.gov identifier NCT00107289) and in accordance with the Health Insurance Portability and Accountability Act. Informed consent was obtained from all individual participants included in the study. Salient eligibility criteria included age >1 year, evidence of evaluable or measurable MIBG-avid disease, and availability of cryopreserved hematopoietic stem cells. Patients with significant renal, cardiac, hepatic, pulmonary, gastrointestinal, and neurologic toxicity were excluded.

MIBG Therapy

All patients were initially treated with a dose of 666 MBq/Kg (18 mCi/kg) ^{131}I-MIBG. Pretreatment saturated solution of potassium iodide and levothyroxine was given for thyroid protection and a urinary catheter was placed and retained while patients remained in the hospital. Patients were monitored clinically and biochemically for toxicity.

A second dose of therapeutic ^{131}I-MIBG was administered if patients: (a) did not experience major toxicity after the first ^{131}I-MIBG infusion; (b) did not experience severe myelosuppression after the first dose; (c) did not require stem cell rescue; and (d) had at least partial response (PR) as defined by the International Neuroblastoma Response Criteria[19] or had an objective improvement in ^{123}I-MIBG scan performed 4–6 weeks after MIBG therapy. The activity of the second ^{131}I-MIBG administration was planned at a dose of 666 MBq/Kg (18mCi/kg) based on the following criteria: estimated absorbed doses from two cumulative ^{131}I-MIBG therapy doses (666 MBq/Kg or 18 mCi/kg each) for liver, kidneys, and lung were less than 30, 20, and 15 Gy, respectively.[20] The estimation of absorbed doses was based on actual calculations of absorbed doses from the first ^{131}I-MIBG post-therapy scans and projections from dosimetry calculations from serial ^{123}I-MIBG scans

performed at follow-up after the first therapy dose. If the estimated absorbed doses to target organs (based on both the actual and projected) were below tolerance doses, the second therapy dose was administered at 666 MBq/Kg or 18 mCi/kg (Fig. 1). Alternately, the administered dose was reduced based on the projected permissible activity.

Post-MIBG therapy—After completing protocol requirements, patients could receive autologous stem cell rescue (ASCR) to reverse myelosuppression as clinically needed. Patients were followed for toxicities until hematopoietic recovery (absolute neutrophil count >500/ul and transfusion-independent platelet count >20,000/ul) was observed.

Pharmacokinetics

Pharmacokinetic studies after ^{131}I-MIBG therapy included: (a) Whole-body counting using an ionization-chamber survey meter (Keithley Model 36100, Keithley Instruments, Inc., Cleveland, OH) calibrated with ^{137}Cs; (b) blood clearance by radioassay of serial blood samples; and (c) whole-body and organ activity measured by conjugate-view whole-body gamma-camera scanning. Blood activity concentrations and gamma camera imaging-derived whole-body and organ activities were used for dosimetry. We compared the whole-body cumulated activities derived from whole-body counting, gamma camera imaging, and combining the counting and imaging data in order to assess the differences in the whole-body cumulated activity derived by these three different approaches.

Whole-body counting—Exposure rate measurements (at surface and at a one-meter distance from the patient) were recorded immediately post-infusion (time 0) and at least once daily while the patient remained in isolation following the ^{131}I-MIBG therapy. Measurements were normalized to the time 0 measurement to yield the corresponding whole-body retention fraction (WBRF) of ^{131}I. WBRFs were fit to a bi-exponential function (in some cases, a mono-exponential function).

Blood sampling and dosimetry—Blood samples were drawn at time 0 and then, 2, ~4, ~8, ~16, ~24, ~48, ~72, ~96, and ~168 h after the first MIBG therapy only. Measured aliquots of blood were assayed in duplicate in a scintillation well counter (LKB Wallach, Inc.) calibrated for ^{131}I and the net count rates converted to activity concentrations in percent of the injected activity per gram (% ID/g). The resulting time-activity concentration data decay-corrected to the time of administration were fit to a bi-exponential function. The fitted biological clearance constants were converted to effective clearance constants by incorporation of the ^{131}I physical decay constant and the blood ^{131}I cumulated activity concentration calculated by analytic integration of the resulting function. The mean blood absorbed dose was calculated by multiplying the blood cumulated activity concentration by the ^{131}I equilibrium dose constant for non-penetrating radiation (i.e., beta particles), assuming complete absorption of the ^{131}I beta particles in blood and ignoring the much smaller ^{131}I gamma-ray absorbed-dose contribution.

Imaging—A Skylight dual-head gamma camera system (Philips Inc., Bothell, WA) was used for all whole-body conjugate (anterior and posterior)-view scanning with high-energy collimators for ^{131}I imaging (photopeak energy window: 364 keV ± 10%) and medium-

energy collimators for ^{123}I imaging (159 keV ± 10%). A calibrated standard of ~250 μCi of either ^{131}I or ^{123}I was included in the field of view for each scan and used to convert the net geometric-mean counts to activity (in μCi) and then % administered activity. Three serial conjugate-view whole-body gamma camera scans were acquired from 48 to 120 hours after ^{131}I-MIBG infusion such that sequential scans were performed at least one day apart (Fig. 2a). Five to seven weeks later, patients were injected with ^{123}I-MIBG (370 MBq/m^2 or 10 mCi/m^2) and underwent conjugate whole-body imaging on the day of injection (2–4 hours) and at approximately 24 and 48 hours post-infusion (Fig. 2b).

Whole-Body and Organ Dosimetry

Regions of interest (ROIs) were manually drawn around the whole body, heart, liver, and lung on the whole-body scans and on the reference standard imaged with the whole-body scans. ROI analyses were performed using a Hermes imaging system (Hermes Medical Solutions, Chicago, IL). ROIs were copied and pasted to all other image sets using software that allowed visualization and linking of multiple image sets. For the whole-body and foregoing normal-organ ROIs, the geometric mean net count rates were converted to activities (kBq) using the standard-derived system calibration factor (cpm/kBq). The resulting non-decay-corrected time-activity data for each organ were fit to bi-exponential functions, which were then integrated to yield the ^{131}I organ cumulated activities (μCi-h/^{131}I μCi administered); for the ^{123}I-MIBG scans, the time-activity data were adjusted to account for the difference in physical half-lives between ^{123}I and ^{131}I. Organ mean absorbed doses for the ^{131}I-MIBG therapy administration and doses projected for the second therapy administration based on the ^{123}I-MIBG time-activity data were calculated using the *OLINDA* dosimetry program.[21] Whole-body and organ masses for the anatomic model in *OLINDA* whose whole-body mass most closely matched that of the patient were scaled in proportion to the patient-to-anatomic model whole-body mass ratio.

Statistical Analyses

The data for ^{131}I-MIBG dosimetry and ^{123}I-MIBG dosimetry were summarized using the median and median absolute deviation (MAD), a non-parametric alternative to standard deviation. The Wilcoxon signed-rank test for paired data was used to test for a significant difference in doses estimated between ^{123}I-MIBG and ^{131}I-MIBG. In order to test for a difference in the variances of ^{123}I-MIBG and ^{131}I-MIBG, a test for a non-zero rank correlation between ^{123}I-MIBG + ^{131}I-MIBG and ^{123}I-MIBG − ^{131}I-MIBG was employed. The Spearman rank correlation was also used to summarize the correlation between estimated organ doses separately within the ^{123}I-MIBG and ^{131}I-MIBG methods. The whole-body and blood clearance data were correlated using the Spearman rank correlation.

RESULTS

Patients and Therapy

Thirty-three patients (19 male and 14 female) received one dose of 666 MBq/kg (18 mCi/kg) ^{131}I-MIBG therapy followed by serial ^{131}I-MIBG scans. Median (± standard deviation, SD) age at first dose was 6.9 ± 3.2 years. Median administered activity for the first injection was 14 ± 7.36 GBq (range 6.07–40 GBq) [388 ± 199 (range 164–1091) mCi]. In all patients

who responded to the first therapy dose, the planned dose for the second treatment was 666 MBq/kg (18 mCi/kg). Nineteen patients received a second ^{131}I-MIBG therapy administration: median 322 ± 186 mCi (range: 166–806) at a median interval of 55 days. Out of the 19 patients, 17 received a second therapy dose at 666 MBq/kg (18 mCi/kg). In 2/19 patients, a dose reduction was needed based on ^{123}I-MIBG dosimetry projections that showed larger than 30 Gy cumulative dose to liver if the second dose was also 666 MBq/kg (18 mCi/kg). The activity for the second administration was reduced by 39% and 58% (from the proposed 18 mCi/kg) ^{131}I-MIBG dose for these two patients to keep the total absorbed dose to liver <30 Gy.

Fourteen of the total 33 patients did not receive a second treatment due to progressive disease or lack of response (n=12), prolonged severe myelosuppression (n=1), or sepsis (n=1) after the first dose.

Toxicities

All patients experienced expected ≥ grade 3 thrombocytopenia after either single or dual tandem MIBG therapy (Table 1) and ≥ grade 3 neutropenia was experienced by 27 and 17 patients in the single or tandem MIBG therapy groups, respectively. Median ± SD post-stem cell rescue times to recovery to absolute neutrophil count (ANC) > 500 was 13 ± 4.6 days for single vs. 13 ± 2.7 days for double MIBG therapy. Median time to transfusion-independent platelet recovery for single vs. double MIBG therapy was 24 ± 4 vs. 23 ± 4.9 days ($p > 0.1$ for both by students t-test). Three patients developed neutropenic sepsis— two after the first MIBG therapy and one after the second. There was no statistical difference in the incidence of toxicities after one or two doses of MIBG therapy ($p > 0.1$ for vomiting and hematopoietic toxicities). Non-hematopoietic toxicities were rare in both single and double MIBG therapy groups. No major organ toxicities were present in any patient, with a median follow-up of 3.3 years (range 2–6.8 years) in 10 surviving patients or until the time of last follow-up in those who expired of disease. Five patients who received two doses survived (median follow-up of 2.5 years (range 2.1–3.6 years) after the second dose, and no organ dysfunction was noted. Following single dose administration, thyroid function tests (TFT) performed at 3–6 months post-administration showed grade I toxicity in 2/11 (18.2%) while for those who received two doses, 16/19 patients had thyroid function tests within the 3- to 6-month follow-up, of which 2/16 had grade I toxicity (12.5%). None of the patients required thyroid hormone supplementation at any time point up to the last follow-up.

Whole-Body Clearance and Dosimetry

The clearance of activity from the body generally followed a bi-exponential function with most (~90%) of the activity cleared with a rapid initial phase and the remainder of the activity clearing more slowly (Fig. 3A, B). Whole-body data for ^{131}I-MIBG estimated by gamma camera imaging only [mean ^{131}I-MIBG residence time of 18.8 (± 6.2) h] was slightly lower than that estimated using WB counting with survey meter [21.3 (± 10.1) h], but it was grossly similar to the estimations derived from the combination of gamma imaging and WB counts data [17.8 (± 6.8 h)] (r=0.88)].

Although the correlation between whole-body ^{131}I residence times derived from the ^{131}I-MIBG and ^{123}I-MIBG scans was poor (r=0.26), the whole-body ^{131}I mean absorbed doses were similar: 0.162 ± 112 mGy/MBq from the ^{131}I-MIBG therapy and 0.141 ± 0.068 mGy/MBq from ^{123}I-MIBG projections.

Blood Clearance

Blood time-activity data were collected only for the first ^{131}I-MIBG therapy administration and followed a bi-exponential function in all cases (n=31). About 80% of blood activity was cleared very rapidly, with a mean half-time of 1.3 ± 0.80 h (range 0.22–3.47 h), with the remainder of the blood activity cleared more slowly, with a mean half-time of 31.7 ± 35.9 h (range 14.4–216 h) (Fig. 3C).

Organ Dosimetry

Estimates of absorbed doses are provided in Table 2. Notable organ-absorbed doses (mean ± SD) in mGy/MBq (rad/mCi) calculated from the first ^{131}I-MIBG therapy administration for liver (the organ with the maximum absorbed dose) were 0.48 ± 0.29 (1.8 ± 1.06); followed by the lungs, 0.41 ± 0.27 (1.50 ± 0.99); heart wall, 0.23 ± 0.20 (0.84 ±0.76); and bone marrow 0.15 ± 0.11 (0.57 ± 0.42). The mean whole-body absorbed dose was 0.16 ± 0.11 mGy/MBq (0.60 ± 0.42 rad/mCi).

^{123}I-MIBG scans-derived projected ^{131}I-MIBG therapy organ absorbed doses for the second therapy administration (mean ± SD) in mGy/MBq (rad/mCi) were: for liver, 0.90 ± 0.57 (3.32 ± 2.10); lungs, 0.46 ± 0.25 (1.72 ± 0.94); heart wall, 0.63 ± 0.38 (2.32 ±1.40); and bone marrow, 0.11 ± 0.06 (0.42 ± 0.24). The mean whole-body absorbed dose was 0.14 ± 0.07 mGy/MBq (0.52 ± 0.25 cGy/mCi or rad/mCi).

The ratios (mean ± SD) of the ^{123}I-MIBG-based estimates to the ^{131}I-MIBG therapy-based organ-absorbed dose estimates were 2.75 ± 1.84 for heart, 1.81 ± 1.95 for lungs, and 0.72 ± 0.54 for bone marrow. The ratio for whole-body doses was 0.869 ± 0.608. The median (range) dose with ^{123}I-MIBG scan estimates were 0.7 mGy/MBq (0.11–2.2), compared to 0.48 mGy/MBq (0.07–1.18) in ^{131}I-MIBG post-therapy imaging for the liver, and 0.52 mGy/MBq (0.10–1.72) compared to 0.20 mGy/MBq (0.02–1.04) for the heart wall, respectively.

Radiation-absorbed doses for the lungs and whole body were not significantly different between the ^{123}I-MIBG scan estimates and ^{131}I-MIBG post-therapy scan estimates (p=0.21 and 0.12, respectively). Collectively for adrenals, brain, kidneys, muscle, pancreas, red marrow, osteogenic cells, skin, spleen, thymus, and thyroid, radiation doses tended to be greater for the ^{131}I-MIBG therapy than for the ^{123}I-MIBG scan estimates. The dose estimates for these organs were derived from OLINDA projections.

The inter-patient variability in estimated radiation doses was significantly greater with ^{123}I-MIBG as compared to ^{131}I-MIBG for both the heart wall [(MAD) 1.50 vs. 0.58, p = 0.005] and the liver (MAD 1.48 vs. 1.20, p = 0.006), while for total body the variability was significantly greater for ^{131}I-MIBG therapy (MAD 0.31 vs. 0.21, p = 0.005). There was no significant difference in variability between ^{123}I-MIBG and ^{131}I-MIBG therapy organ-

absorbed doses for the lungs. The variability among the combined set of organs (above) was consistently larger in ^{131}I-MIBG post-therapy scan estimates than in ^{123}I-MIBG scan projections (MAD 0.39 vs. 0.21).

The correlation between ^{123}I-MIBG and ^{131}I-MIBG therapy organ-absorbed doses was low, with coefficient value (r) 0.30 for heart wall and liver, 0.60 for lung, and 0.52 for total body. The correlation was also low (r=0.40–0.60 range) for dose estimations to other organs between ^{123}I-MIBG and ^{131}I-MIBG. A moderate positive inter-patient correlation was seen for dose estimates for lung, liver, heart wall, and whole-body exposures (r=0.52 – 0.81) for ^{123}I-MIBG and also ^{131}I-MIBG post-therapy scan organ-absorbed doses (r=0.76 – 0.91). The inter-patient correlation tended to be high between dose estimates for each of the other organs also (r= 0.723–0.996 range for ^{123}I-MIBG and r=0.802–1.00 for ^{131}I-MIBG post-therapy).

DISCUSSION

Although ^{131}I-MIBG therapy has been used for a number of years for treatment of neuroendocrine tumors and neuroblastoma, response rates for currently used activities remain sub-optimal. In neuroblastoma, metastasis to bone marrow occurs in most patients, and hematopoietic stem cells harvesting and banking is increasingly being done in anticipation of infusing them to reverse the myelosuppression that may be associated with high-dose chemotherapy regimens and also high-dose MIBG therapy.[22] Thus, as opposed to myelosuppression, toxicity to non-hematopoietic organs is now dose-limiting.

Dosimetry studies to date have primarily used only whole-body and red marrow-absorbed dose estimates to plan ^{131}I-MIBG therapy administrations, generally considering blood doses as limiting. Monsieurs et al showed the feasibility of using pre-therapy ^{123}I-MIBG imaging for predicting whole-body doses for ^{131}I-MIBG,[12] but only whole-body dosimetry was calculated as opposed to individual organ dosimetry and only two imaging time points up to 24 h post-injection (p.i.) were used for ^{123}I-MIBG estimations. Other methods such as whole-body counting with survey meter[23] or use of whole-body retained activity to estimate maximum 4 Gy total absorbed dose for two ^{131}I-MIBG therapy administrations[13] have also shown large variations.

Assessment of individual organ doses, as opposed to previously used whole-body absorbed doses only, would help individualize therapy; in particular, repeat treatments with high-dose ^{131}I-MIBG would allow for maximizing activity administration while keeping absorbed doses to individual critical organs such as lung, liver, and kidney within tolerance limits. As stem cell support for marrow toxicity is available, organ toxicity rather than marrow toxicity is of higher concern in these patients. We therefore evaluated ^{123}I-MIBG imaging for organ and whole-body radiation dose estimation for planning the dose for the second ^{131}I-MIBG therapy.

Our study shows that, using ^{123}I-MIBG imaging, organ dosimetry is practical and allows for treatment planning to prevent major side effects to normal organs. There was no significant additional or incremental non-hematologic (organ) toxicity in patients who received second

therapy based on our dosimetric estimates. In two cases, the organ doses were over the maximum allowed radiation limits with two full high-dose administrations (666 MBq/kg or 18 mCi/kg) of the ^{131}I-MIBG therapy. In those two cases, the activity for the second treatment was reduced based on estimations with ^{123}I-MIBG imaging. In both cases, the limiting organ was liver and required 39% and 58% lower administered activities from the preplanned dose (666 MBq/kg or 18 mCi/kg) for the second ^{131}I-MIBG administration. Follow-up in these patients after two therapies showed no signs of liver dysfunction up to the last follow-up, to a median follow-up of 2.5 years. Marrow toxicity, as expected, was seen in a majority of the patients with this treatment, consistent with the general experience with high-dose ^{131}I-MIBG therapy. However, no significant difference was evident in the marrow toxicity profile for those who received only a single dose vs. those who received a second ^{131}I-MIBG therapy.

The radiation doses estimated by ^{123}I-MIBG vs. ^{131}I-MIBG post-therapy scanning showed significant differences, with the radiation-absorbed doses to liver, lungs, and heart generally greater with ^{123}I-MIBG. The overall estimates with ^{123}I-MIBG vs. ^{131}I-MIBG scan-derived absorbed doses were about twice for these organs, with an overall average ^{123}I-MIBG to ^{131}I-MIBG dose ratio of 1.9 (1.1–2.7). For other organ systems including marrow and whole body, however, dose estimates were generally lower for ^{123}I-MIBG, with an average ratio of 0.78 (0.65–0.97). There was a large variation in the individual organ dosimetry estimates for both methods, which is expected due to individual differences likely related to biological clearance. Technical and practical limitations that influence accurate estimations may contribute to these differences. Liver and heart wall RAD estimates were significantly greater for ^{123}I-MIBG compared to ^{131}I-MIBG estimates ($p < 0.001$ for both the liver and heart wall). While the exact reason for this is not entirely clear, it may be related to technical aspects. In five out of the eight cases with higher cardiac uptake on the ^{123}I-MIBG, there was disease in the mediastinum and prominent uptake in the liver that could have contributed to the estimations from the ROI placements. It is likely that higher visibility of lesions on post-therapy scans allows for placement of ROI away from the lesion site. This, however, does not entirely explain the discrepancy in other cases. Additionally, the fact that dose estimates were variable and generally higher for key major organs than those derived from the first ^{131}I-MIBG administration may reflect therapy-induced changes in MIBG pharmacokinetics. Alternatively, the ^{123}I-MIBG-derived ^{131}I-MIBG doses may be overestimates of the actual ^{131}I-MIBG doses related simply to methodology; i.e., the earlier times post-administration at which ^{123}I must be imaged than longer-lived ^{131}I yield higher activity measurements. An additional limitation for ^{123}I-MIBG imaging is restricting imaging times up to 48 hours post-administration due to its relatively short half-life. Certain assumptions—specifically, a bi-exponential time-activity function—are therefore required to extrapolate the time-activity data in order to derive the dose estimates that may contribute to variations.

The correlation of whole-body clearances for ^{131}I-MIBG and ^{123}I-MIBG is limited due to the fact that data were collected at a later time point p.i. for the ^{131}I-MIBG than for the ^{123}I-MIBG. The terminal total-body clearance half-times for ^{123}I-MIBG could not be determined precisely due to early imaging p.i. Clinical and logistical considerations restricted collection of time-activity data by imaging to 2 to 6 days post-^{131}I-MIBG therapy administration vs.

earlier time points. Similarly, the WB count data and ^{123}I-MIBG whole-body scanning data is for only 1 to 2 days post-^{123}I-MIBG administration. This is probably a major factor in the differences seen as the assessment for ^{131}I-MIBG starts later post-injection, which may affect the estimates on the clearance and residence times. Correspondingly, for ^{123}I-MIBG, the later time points are not measurable, thereby limiting the assessment of second phase of clearance which may again affect the estimates for clearance and residence times. An additional possible reason is that the differences in the mass of the MIBG in the infusions, which are significantly lower for ^{123}I-MIBG than for ^{131}I-MIBG (approximately 0.5 mg vs. 20–25 mg, respectively), may impact the kinetics.

Previous studies using different techniques have also noted that dose estimates derived from diagnostic scans may vary from those estimated from the images for therapy administrations,[14] with the possibility of under-dosing in 65% of patients based on diagnostic scan estimates. High variation is also seen in predicting body and tumor doses from therapy using diagnostic imaging.[15, 16]

While a number of different methodologies have been used, there are some limitations to all. Use of low-activity ^{131}I-MIBG imaging for dosimetry has been described; however, the image quality is suboptimal and the radiation dose received from ^{131}I is higher. The radiation dose from ^{131}I-MIBG imaging, as compared to ^{123}I-MIBG imaging, is an important consideration, especially in children. Since the majority of these patients are imaged clinically with ^{123}I-MIBG, assessment of dosimetry at the same time would be more practical and convenient. Furthermore, due to high activity, gamma camera dead-time (i.e., count-loss), and radiation safety considerations, ^{131}I-MIBG post-therapy imaging cannot be performed at early time points, which limits estimations. Additionally, no gold standard exists to determine the accuracy of the ^{131}I-MIBG dose estimates.

^{123}I-MIBG is FDA-approved and is the recommended standard imaging modality for NB. Currently, there is limited data on the use of ^{123}I-MIBG imaging for estimating individual organ dosimetry in planning repeat MIBG therapy. Our study has shown the feasibility of the use of serial ^{123}I-MIBG scanning for estimating absorbed doses to organs for repeat high-dose treatment planning.

It can be thought that projected ^{123}I-MIBG-derived ^{131}I-MIBG doses may either be the actual ^{131}I-MIBG organ-absorbed doses or an overestimate of those doses, in which case the activity administered would be lower than necessary and well with within safe limits. Conceivably, the ^{123}I-MIBG-derived dose estimates were reasonably accurate and safe in view of the lack of significant toxicities in the patients. The high-dose second ^{131}I-MIBG therapy based on ^{123}I-MIBG dose estimates was well tolerated by all patients and no serious adverse events or organ-related toxicities were observed during the follow-up in any patient. Based on the clinical data, it appears that ^{123}I-MIBG-derived ^{131}I-MIBG organ-absorbed dose represents a “safe” (i.e., conservative) basis for planning a second ^{131}I-MIBG high-dose therapy.

CONCLUSIONS

Both ^{131}I-MIBG post-therapy and ^{123}I-MIBG imaging yielded variable organ doses. However, ^{123}I-MIBG-based dosimetry yielded a more conservative estimate of maximum allowable activity for individual organs as compared to ^{131}I-MIBG, and would be a suitable method for planning and limiting organ toxicity with repeat high-dose therapies.

Acknowledgments

The authors thank nuclear medicine nurses Amabelle Lindo and Louise Harris for their help in patient management, and Leah Bassity for editorial support.

References

1. Brisse HJ, McCarville MB, Granata C, et al. Guidelines for imaging and staging of neuroblastic tumors: consensus report from the International Neuroblastoma Risk Group Project. Radiology. 2011; 261:243–257. [PubMed: 21586679]
2. Matthay KK, Shulkin B, Ladenstein R, et al. Criteria for evaluation of disease extent by (^{123})I-metaiodobenzylguanidine scans in neuroblastoma: a report for the International Neuroblastoma Risk Group (INRG) Task Force. Br J Cancer. 2010; 102:1319–1326. [PubMed: 20424613]
3. Monclair T, Brodeur GM, Ambros PF, et al. The International Neuroblastoma Risk Group (INRG) staging system: an INRG Task Force report. J Clin Oncol. 2009; 27:298–303. [PubMed: 19047290]
4. Cohn SL, Pearson AD, London WB, et al. The International Neuroblastoma Risk Group (INRG) classification system: an INRG Task Force report. J Clin Oncol. 2009; 27:289–297. [PubMed: 19047291]
5. Wilson JS, Gains JE, Moroz V, et al. A systematic review of ^{131}I-meta iodobenzylguanidine molecular radiotherapy for neuroblastoma. Eur J Cancer (Oxford, England: 1990). 2014; 50:801–815.
6. van Santen HM, de Kraker J, van Eck BL, et al. High incidence of thyroid dysfunction despite prophylaxis with potassium iodide during (131)I-meta-iodobenzylguanidine treatment in children with neuroblastoma. Cancer. 2002; 94:2081–2089. [PubMed: 11932913]
7. Matthay KK, Tan JC, Villablanca JG, et al. Phase I dose escalation of iodine-131-metaiodobenzylguanidine with myeloablative chemotherapy and autologous stem-cell transplantation in refractory neuroblastoma: a new approaches to Neuroblastoma Therapy Consortium Study. J Clin Oncol. 2006; 24:500–506. [PubMed: 16421427]
8. Modak S, Zanzonico P, Carrasquillo JA, et al. Arsenic trioxide as a radiation sensitizer for ^{131}I-metaiodobenzylguanidine therapy: results of a phase II study. J Nucl Med. 2016; 57:231–237. [PubMed: 26742708]
9. DuBois SG, Chesler L, Groshen S, et al. Phase I study of vincristine, irinotecan, and (1)(3)(1)I-metaiodobenzylguanidine for patients with relapsed or refractory neuroblastoma: a new approaches to neuroblastoma therapy trial. Clin Cancer Res. 2012; 18:2679–2686. [PubMed: 22421195]
10. Johnson K, McGlynn B, Saggio J, et al. Safety and efficacy of tandem ^{131}I-metaiodobenzylguanidine infusions in relapsed/refractory neuroblastoma. Pediatr Blood Cancer. 2011; 57:1124–1129. [PubMed: 21495159]
11. Monclair T, Brodeur GM, Ambros PF, et al. The International Neuroblastoma Risk Group (INRG) staging system: an INRG Task Force report. J Clin Oncol. 2009; 27:298–303. [PubMed: 19047290]
12. Monsieurs M, Brans B, Bacher K, et al. Patient dosimetry for ^{131}I-MIBG therapy for neuroendocrine tumours based on ^{123}I-MIBG scans. Eur J Nucl Med Mol Imaging. 2002; 29:1581–1587. [PubMed: 12458391]
13. Buckley SE, Saran FH, Gaze MN, et al. Dosimetry for fractionated (131)I-mIBG therapies in patients with primary resistant high-risk neuroblastoma: preliminary results. Cancer Biother Radiopharm. 2007; 22:105–112. [PubMed: 17627418]

14. Fielding SL, Flower MA, Ackery D, et al. Dosimetry of iodine 131 metaiodobenzylguanidine for treatment of resistant neuroblastoma: results of a UK study. Eur J Nucl Med. 1991; 18:308–316. [PubMed: 1936038]
15. Lashford LS, Lewis IJ, Fielding SL, et al. Phase I/II study of iodine 131 metaiodobenzylguanidine in chemoresistant neuroblastoma: a United Kingdom Children's Cancer Study Group investigation. J Clin Oncol. 1992; 10:1889–1896. [PubMed: 1453204]
16. Matthay KK, Panina C, Huberty J, et al. Correlation of tumor and whole-body dosimetry with tumor response and toxicity in refractory neuroblastoma treated with (131)I-MIBG. J Nucl Med. 2001; 42:1713–1721. [PubMed: 11696644]
17. Seo Y, Gustafson WC, Dannoon SF, et al. Tumor dosimetry using [^{124}I]m-iodobenzylguanidine microPET/CT for [^{131}I]m-iodobenzylguanidine treatment of neuroblastoma in a murine xenograft model. Mol Imaging Biol. 2012; 14:735–742. [PubMed: 22382618]
18. Huang SY, Bolch WE, Lee C, et al. Patient-specific dosimetry using pretherapy [^{124}I]m-iodobenzylguanidine ([^{124}I]mIBG) dynamic PET/CT imaging before [^{131}I]mIBG targeted radionuclide therapy for neuroblastoma. Mol Imaging Biol. 2015; 17:284–294. [PubMed: 25145966]
19. Brodeur GM, Pritchard J, Berthold F, et al. Revisions of the international criteria for neuroblastoma diagnosis, staging, and response to treatment. J Clin Oncol. 1993; 11:1466–1477. [PubMed: 8336186]
20. Emami B, Lyman J, Brown A, et al. Tolerance of normal tissue to therapeutic irradiation. Int J Radiat Oncol Biol Phys. 1991; 21:109–122. [PubMed: 2032882]
21. Stabin MG, Sparks RB, Crowe E. OLINDA/EXM: the second-generation personal computer software for internal dose assessment in nuclear medicine. J Nucl Med. 2005; 46:1023–1027. [PubMed: 15937315]
22. Grupp SA, Cohn SL, Wall D, et al. Collection, storage, and infusion of stem cells in children with high-risk neuroblastoma: saving for a rainy day. Pediatr Blood Cancer. 2006; 46:719–722. [PubMed: 16429413]
23. Buckley SE, Chittenden SJ, Saran FH, et al. Whole-body dosimetry for individualized treatment planning of 131I-MIBG radionuclide therapy for neuroblastoma. J Nucl Med. 2009; 50:1518–1524. [PubMed: 19713562]

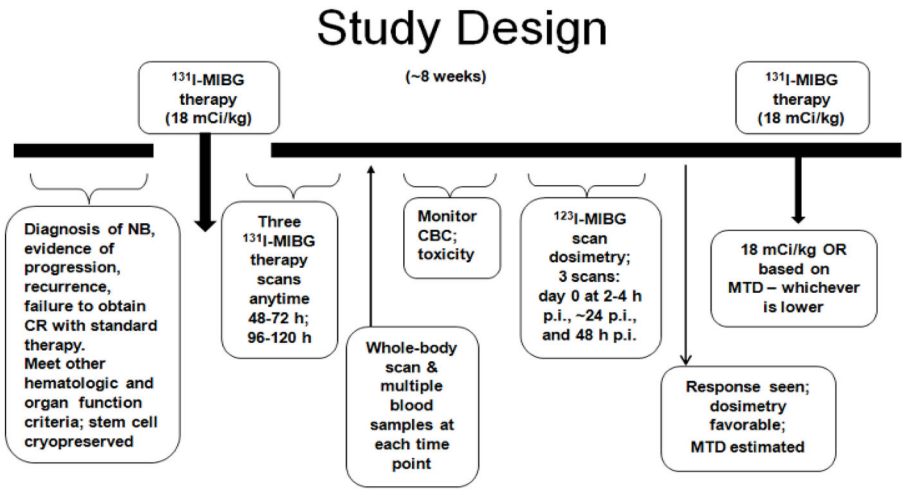

Figure 1.
Study schema.

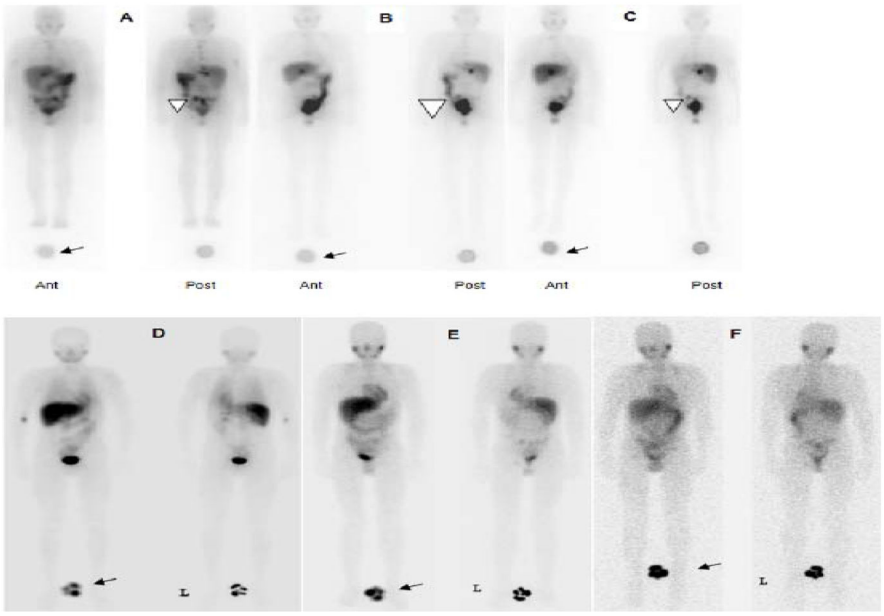

Figure 2.

^{131}I-MIBG post-therapy scans: anterior and posterior whole-body images performed at 48 h (A), 72 h (B), and 120 h (C) post-injection. A reference standard was included for imaging at all time points (arrows). Images show physiologic uptake in liver, spleen, GI tract, kidneys, and bladder. Uptake is also seen in the left pelvic lesion (arrow head). ^{123}I-MIBG scans: anterior and posterior whole-body images performed at 1.5 h (D), 24 h (E), and 48 h (F) post-injection. A reference standard was included for imaging at all time points (arrows). Physiologic uptake is seen in the heart, liver, spleen, GI tract, and bladder.

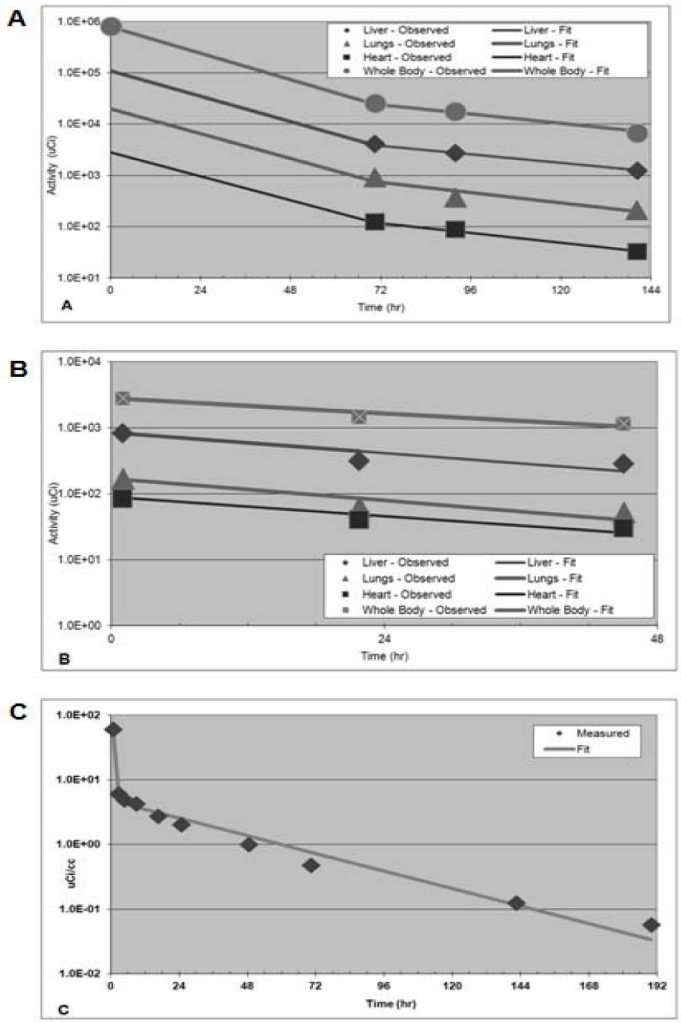

Figure 3.

Time-activity clearance curves for the whole body and organs for ^{131}I -MIBG (A) and ^{123}I-MIBG (B). Blood clearance time-activity curve for ^{131}I-MIBG (C).

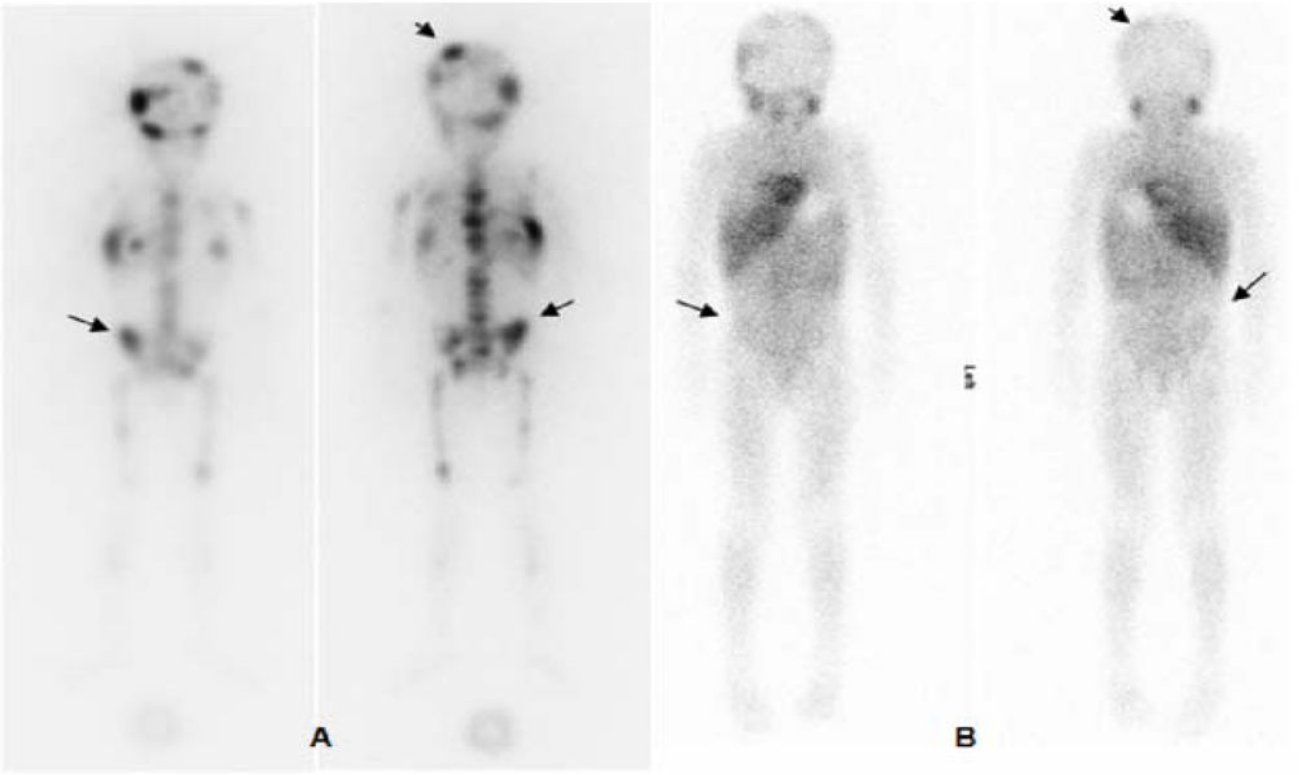

Figure 4.

^{123}I-MIBG pre-therapy (A) and post-therapy (B) scans: anterior and posterior whole-body images performed at 24 h post-injection. Images show multiple abnormal foci of uptake in the axial and appendicular skeleton that are resolved (arrows) or decreased (arrow heads) in the post-therapy scan.

Table 1

Patient-related toxicities *

	After first dose (n = 33)				After second dose (n = 19)			
Toxicity	**Grade 1**	**Grade 2**	**Grade 3**	**Grade 4**	**Grade 1**	**Grade 2**	**Grade 3**	**Grade 4**
Elevated AST	19	5	3	0	6	4	1	0
Elevated ALT	21	6	1	0	6	3	2	0
Hyperbilirubinemia	1	0	0	0	0	0	0	0
Vomiting	8	5	1	0	7	0	0	0
Anemia	3	12	16	2	0	5	14	0
Lymphopenia	0	1	3	29	0	2	4	13
Neutropenia	0	6	16	11	0	1	7	11
Thrombocytopenia	0	0	6	27	0	0	0	19
Sepsis	0	2	0	0	0	1	0	0

* Common Terminology Criteria for Adverse Events 3.0 (https://ctep.cancer.gov/protocoldevelopment/electronic_applications/docs/ctcaev3.pdf)

Abbreviations: ALT: alanine transferase; AST: aspartame transferase

Table 2

Estimated organ dosimetry from ^{123}I-MIBG and ^{131}I-MIBG

	rad/mCi (cGy/mCi)				mGy/Mbq			
	^{123}I-MIBG		^{131}I-MIBG		^{123}I-MIBG		^{131}I-MIBG	
	Mean	**SD**	**Mean**	**SD**	**Mean**	**SD**	**Mean**	**SD**
Adrenals	0.539	0.221	0.645	0.423	0.146	0.060	0.174	0.114
Brain	0.341	0.174	0.521	0.377	0.092	0.047	0.141	0.102
Heart wall	2.285	1.396	0.831	0.758	0.618	0.377	0.225	0.205
Kidneys	0.587	0.673	0.606	0.409	0.159	0.182	0.164	0.111
Liver	3.274	2.080	1.803	1.063	0.885	0.562	0.487	0.287
Lungs	1.694	0.930	1.498	0.997	0.458	0.251	0.405	0.269
Muscle	0.492	0.577	0.557	0.390	0.133	0.156	0.151	0.105
Pancreas	0.566	0.241	0.656	0.444	0.153	0.065	0.177	0.120
Red marrow	0.409	0.234	0.566	0.428	0.111	0.063	0.153	0.116
Osteogenic cells	0.704	0.354	1.024	0.798	0.190	0.096	0.277	0.216
Skin	0.330	0.184	0.474	0.343	0.089	0.050	0.128	0.093
Spleen	0.428	0.208	0.584	0.415	0.116	0.056	0.158	0.112
Thymus	0.414	0.197	0.567	0.398	0.112	0.053	0.153	0.108
Thyroid	0.387	0.198	0.576	0.413	0.105	0.054	0.156	0.112
Total body	0.521	0.251	0.599	0.413	0.141	0.068	0.162	0.112